THE ASTROPHYSICAL JOURNAL, 165:57–66, 1971 April 1

VISUAL INTRINSIC POLARIZATION AND INFRARED EXCESS OF COOL STARS

H. M. DYCK
Kitt Peak National Observatory

W. J. FORREST AND F. C. GILLETT*
University of California, San Diego

W. A. STEIN*
University of California, San Diego, and University of Minnesota

R. D. GEHRZ* AND N. J. WOOLF*
University of Minnesota

AND

S. J. SHAWL*
University of Texas
Received 1970 October 6; revised 1970 November 6

ABSTRACT

Observations of intrinsic polarization and infrared photometry of approximately sixty late-type stars have been combined. A relation is shown to exist in the data between measured intrinsic polarization and amount of infrared excess at 11 μ. A theory is derived which explains this relationship and which shows that polarization and infrared excess are related through the scattering and absorption optical depths of a circumstellar cloud of solid particles. The characteristics of the scattering particles are discussed by applying the theory to the data.

I. INTRODUCTION

It is well known now that many late-type stars exhibit polarization intrinsic to the objects themselves and independent of interstellar polarization. Observations of the characteristics of this intrinsic polarization have been made and discussed by Serkowski (1966*a*, *b*), Kruszewski, Gehrels, and Serkowski (1968), and Dyck (1968). In these investigations considerable information has been obtained about the wavelength dependence and time dependence of the polarization.

It has been suggested that the intrinsic polarization of cool stars is due to scattering by solid particles in the atmospheres or in envelopes surrounding these stars. Donn *et al.* (1966) suggested that the polarization arose from absorption by aligned graphite grains. The particles were thought to be aligned by magnetic fields of the cool stars. Kruszewski *et al.* (1968) derived a simple model showing that polarization need not be produced by aligned particles but that scattering of light by particles in an asymmetric envelope was sufficient to produce the observed results. An alternative explanation has been proposed by Harrington (1969). A major source of opacity in late-type stars is scattering in their atmospheres. The combination of scattering, some absorption, and a Planck function that changes rapidly with wavelength produces strongly polarized radiation from all but the center of the stellar disk. Any asymmetrical shape of the star, or the presence of large convective cells, could also produce polarized starlight.

Recently, infrared observations have shown that solid particles are common around

* Visiting Astronomer, Kitt Peak National Observatory, which is operated by the Association of Universities for Research in Astronomy, Inc., under contract with the National Science Foundation

stars. Woolf and Ney (1969) have attributed the emission peak at $\lambda = 10\ \mu$ in M stars (Gillett, Low, and Stein 1968) to metallic silicates. It is expected that graphite particles would condense out of gas surrounding carbon-rich stars (Hoyle and Wickramasinghe 1962), and the question of the various expected condensates as a function of the oxygen-to-carbon ratio has recently been investigated by Gilman (1969).

The observations of infrared emission from solids surrounding cool stars clearly strengthen considerably the suggestions that polarization is due to scattered light from particles. The existence of a possible correlation between cool stars which exhibit intrinsic polarization and cool stars with observed infrared excesses was suggested by Kruszewski, Coyne, and Gehrels (1969).

During the observing period from 1969 October–1970 June a large number of cool stars were observed at Kitt Peak National Observatory at infrared wavelengths in two independent programs by Gillett and Stein and by Gehrz and Woolf. Many of the stars observed were stars that were also being observed for intrinsic polarization by Dyck. This discussion describes the results of combining those data for approximately sixty cool stars and shows that a correlation does exist.

II. OBSERVATIONS

The infrared observations described here were carried out at Kitt Peak National Observatory with a photometric system containing four passbands: The spectral bandpasses used were $\lambda_0 = 3.5\ \mu$ with $\Delta\lambda = 1.0\ \mu$, $\lambda_0 = 4.9\ \mu$ with $\Delta\lambda = 1.0\ \mu$, $\lambda_0 = 8.4\ \mu$ with $\Delta\lambda = 0.8\ \mu$, and $\lambda_0 = 11.0\ \mu$ with $\Delta\lambda = 2\ \mu$. The calibration of the photometric data is tabulated in Table 1, in which the flux in units of watts $cm^{-2}\ \mu^{-1}$ and in units of watts $m^{-2}\ Hz^{-1}$ is shown for zero magnitude at each wavelength. Magnitudes are designated by λ_0 enclosed in brackets—for example, [3.5 μ]. The observing procedure included the usual technique of dual-beam chopping common to all infrared measurements. Most of the stars observed were relatively bright, and thus only short integrating times were necessary.

The polarization data were obtained partly from older literature (Serkowski 1966*a*, *b*, 1969; Coyne and Kruszewski 1968; Kruszewski *et al.* 1968; Dyck 1968; Shawl 1969), but the majority have been measured since 1969 October at KPNO and are described by Dyck and Sandford (1971) and Dyck and Jennings (1971). A few unpublished data taken by Shawl have also been included. The polarimeter used for the new observations is described by Dyck and Sandford (1971). Only tabulated data from other polarimetry systems have been used, and these only when a sufficient number of interstellar-polarization objects were measured in common to determine the compatibility of the systems. Since data obtained in the $B(0.44\ \mu)$ and $V(0.55\ \mu)$ bands comprise most of the observations, numerical computations using the amounts of polarization have been restricted to these two colors for the sake of homogeneity.

TABLE 1

ABSOLUTE CALIBRATION OF THE PHOTOMETRIC INFRARED OBSERVATIONS

		Flux for Zero Magnitude		
$\lambda_0(\mu)$	$\Delta\lambda(\mu)$	F_λ(W $cm^{-2}\ \mu^{-1}$)	F_ν(W $m^{-2}\ Hz^{-1}$)	ν_0(Hz)
3.5.....	1.0	7.1×10^{-15}	2.9×10^{-24}	8.6×10^{13}
4.9.....	1.0	2.0×10^{-15}	1.6×10^{-24}	6.1×10^{13}
8.4.....	0.8	2.45×10^{-16}	5.8×10^{-25}	3.6×10^{13}
11.0.....	2.0	8.6×10^{-17}	3.5×10^{-25}	2.7×10^{13}

III. RESULTS

The results of combining the infrared and polarization data are tabulated in Table 2. The quantities tabulated include the star designation, the average measured polarization, the average deviation of measured polarization, the 3.5-μ observed magnitude designated [3.5 μ], and the magnitude differences, [4.9 μ] − [3.5 μ], [8.4 μ] − [3.5 μ], and [11.0 μ] − [3.5 μ].

The calibration of the infrared magnitude system in units of flux was shown in Table 1; in general, large signals were observed from most stars so that statistical errors were small. Calibrations on stars of known brightness and corrections for differential extinction were made several times during each night's observation. As a result of these procedures, it is estimated that errors of approximately ± 0.1 mag can be assigned to each measured infrared magnitude.

The average polarization is simply the time-averaged amount of polarization in B and V computed from

$$\langle P \rangle = \frac{1}{N} \sum_{i=1}^{N} P(t_i) ,$$

where $P(t)$ is the amount of polarization at time t and N is the number of nights on which observations were made. The average deviation of P is defined by

$$\langle |\Delta P| \rangle = \frac{1}{N} \sum_{i=1}^{N} |P(t_i) - \langle P \rangle|$$

and therefore is a measure of the amplitude of the polarization variation. Both of these quantities will be affected by the completeness of the set of observations and the uniformity in time with which the data were collected and will therefore have unavoidable scatter in a plot of intrinsic polarization against infrared color. The average polarization may, in addition, be affected by a large interstellar component for those objects in the galactic plane, and the amount of the contribution will be difficult to estimate. No attempt has been made to estimate the maximum amount of polarization because of the generally nonsystematic way in which the data have been taken.

As a result of the combination of infrared data and polarization data, a correlation was found to exist between infrared excess in terms of magnitude difference [11.0 μ] − [3.5 μ] and averaged measured polarization $\langle P \rangle$. These data are plotted in Figure 1 for all of the cool stars measured in common. It is clear from Figure 1 that at the very least an upper bound in the plot exists above which no stars are found. That is, no stars with measurable intrinsic polarization are found which do not have an infrared excess at 11 μ. The only possible exception to this is the star 119 Tau that may lie slightly in the area in which no other stars are found. A plot of the same data was made for only those stars with galactic latitude $|b^{II}| > 20°$, in order to eliminate any possible contamination by stars with interstellar polarization. The diagram under these conditions remained almost completely unchanged except that the possible one exception to the upper bound in Figure 1 (119 Tau) was removed. 119 Tau has a galactic latitude $b^{II} = -8°$.

The qualitative interpretation of the results shown in Figure 1 is clear. If intrinsic polarization of optical-wavelength light is observed from a star, then that star exhibits an infrared excess at $\lambda = 11$ μ. The reverse statement is not so strong. That is, if infrared excess is observed, then most, but not all, stars show intrinsic polarization.

IV. DISCUSSION

The data presented here are open to three possible interpretations. The polarization may be explained by (1) atmospheric scattering, (2) circumstellar scattering by gas, or (3) circumstellar scattering by dust.

TABLE 2

AVERAGE MEASURED POLARIZATION AND INFRARED DATA FOR THE STARS IN THIS STUDY

HD	Name	Spectral Type	b^{II}(°)	$\langle P \rangle$	$\langle \lvert \Delta P \rvert \rangle$	[3.5]	[4.9]−[3.5]	[8.4]−[3.5]	[11.0]−[3.5]
			Giants and Supergiants						
14528	S Per	M3e Ia	− 2	5.8	0.50	+0.68	−0.77	−1.73	−2.97
17491	Z Eri	M4 III	−59	0.9	0.28	+0.26	+0.17	−0.08	−1.10
18884	α Cet	M1.5 III	−46	0.1	0.03	−1.81	+0.22	+0.18	−0.05
19058	ρ Per	M3 II–III	−17	0.1	0.08	−2.12	+0.12	−0.03	−0.16
36389	119 Tau	M2 Ib	− 8	1.2	0.26	−1.19	+0.17	+0.12	−0.16
39801	α Ori	M2 Iab	− 9	0.3	0.08	−4.45	+0.14	−0.33	−1.07
42475	TV Gem	M1 Ia	+ 2	2.6	0.22	+0.62	−0.21	−0.82	−1.89
42543	BU Gem	M2 Iab	+ 2	2.1	0.18	+0.74	+0.01	−0.53	−1.69
42995	η Gem	M3 II	+ 2	0.0	0.04	−1.65	+0.21	+0.08	−0.09
44478	μ Gem	M3 III	+ 4	0.1	...	−2.09	...	...	+0.05
44537	ψ^1 Aur	K5 Ib	+16	0.5	0.16	+0.2	...	...	+0.4
50877	o^1 CMa	M0 Iab	−10	0.2	...	−0.04	+0.25	+0.04	−0.19
58061	VY CMa	M3e	− 5	14.3	0.8	−3.2	−1.0	−2.4	−3.4
78712	RS Cnc	M6 Ib–II	+42	0.5	0.20	−1.95	+0.21	−0.34	−1.10
86663	π Leo	M2 III	+45	0.0	...	+0.21	+0.57	+0.16	+0.06
89758	μ UMa	M0 III	+56	0.1	...	−0.95	+0.31	+0.08	−0.16
94705	VY Leo	M5 III	+56	0.1	0.04	−0.96	+0.35	+0.06	−0.28
95689	α UMa	K0 III	+51	0.1	...	−0.80	+0.09	−0.08	−0.08
97778	72 Leo	M2 III	+68	0.1	...	−0.27	+0.29	+0.01	−0.11
98118	75 Leo	M0 IIIb	+56	0.1	...	+1.19	+0.22	+0.04	−0.18
103681	Z UMa	M5e III	+58	1.0	0.45	+0.19	−0.17	−0.57	−0.93
107397	RY UMa	M3e III	+56	1.5	0.38	+2.17	+0.30	−0.73	−1.71
112300	δ Vir	M3 III	+66	0.1	...	−1.38	+0.12	−0.01	−0.25
113866	40 Com	M5 III	+84	0.1	...	−0.37	+0.27	−0.06	−0.25
115898	VCVn	M4–M6e	+71	3.7	1.30	+0.86	−0.08	−1.25	−2.28
126327	RX Boo	M8e	+69	0.9	0.38	−2.33	+0.01	−0.47	−1.32
132813	RR UMi	M5 III	+47	0.0	0.04	−0.94	+0.27	+0.03	−0.14
139216	τ^4 Ser	M5 IIb–IIIa	+48	0.7	0.21	−1.25	+0.14	−0.23	−0.83
144205	X Her	M6	+47	0.8	0.45	−1.64	+0.09	−0.49	−1.31
148478	g Her	M6 III	+44	0.4	0.12	−2.40	+0.12	−0.18	−0.39
...	UY Sct	M4 Ia–Iab	− 2	3.0	0.64	+0.33	−0.22	−0.76	−2.72
156014	α Her	M5 Ib–II	+28	0.1	...	−3.69	+0.21	−0.11	−0.37
172380	XY Lyr	M4–5 Ib–II	+19	0.1	...	−0.46	+0.20	+0.10	−0.23
175588	δ^2 Lyr	M4 II	+15	0.1	...	−1.45	+0.37	...	−0.21

TABLE 2—*Continued*

HD	Name	Spectral Type	b^{II} (°)	$\langle P \rangle$	$\langle \lvert \Delta P \rvert \rangle$	[3.5]	[4.9−[3.5]	[8.4]−[3.5]	[11.0]−[3.5]
			Giants and Supergiants—*Continued*						
175865.....	R Lyr	M4–M5	+18	0.1	...	−2.23	+0.28	0.00	−0.12
...	NML Cyg	M6 III	− 2	13.4	1.39	−1.93	−1.11	−3.24	−3.84
206936.....	μ Cep	M2 Ia	+ 5	1.5	0.52	−2.3	+0.16	−0.48	−1.86
212466.....	RW Cep	K0 0b	− 1	2.8	0.50	+1.51	−0.11	−1.18	−2.91
217906.....	β Peg	M2–3 II–III	−29	0.0	0.05	−2.22	+0.03	+0.01	−0.10
			Mira-Type Variables						
14386.....	o Cet	M5.5e	−58	0.7	0.28	−3.49	−0.32	−1.10	−2.14
39816.....	U Ori	M6.5e	− 3	1.1	0.27	−1.37	−0.29	−0.74	−1.63
69243.....	R Cnc	M6.5e	+74	1.0	0.32	−1.16	−0.35	−0.78	−1.40
64748.....	R Leo	M7e	+44	0.8	0.28	−3.17	−0.22	−0.75	−1.48
117287.....	R Hya	M6.5e	+39	0.7	0.18	−3.05	−0.06	−0.55	−1.32
120285.....	W Hya	M8e	+32	0.9	0.22	−3.76	−0.53	−0.84	−1.69
128609.....	R Boo	M4.5e	+67	0.9	0.34	+1.26	−0.16	−0.55	−1.00
136753.....	S CrB	M6.5e	+57	0.9	0.15	−0.74	−0.45	−1.44	−2.38
148206.....	U Her	M6.5e	+40	2.0	1.00	−0.78	−0.33	−0.89	−1.81
187796.....	χ Cyg	S7, 2e or M7	+ 3	1.1	0.55	−2.25	−0.32	−0.96	−1.75
			Carbon Stars						
31996.....	R Lep	C7, 6e	−31	2.1	0.28	−0.60	−0.42	−1.19	−1.94
32736.....	W Ori	C5, 3	−23	0.3	0.08	−0.72	+0.39	−0.52	−1.02
92839.....	VY UMa	C6, 3	+45	0.0	0.09	+0.24	+0.08	−0.42	−0.63
...	V Hya	C6, 3e	+34	1.5	1.03	−1.81	−0.51	−1.75	−2.29
108105.....	SS Vir	C6, 3e	+63	0.4	0.23	+0.17	+0.29	−0.73	−1.16
141826.....	V CrB	C6, 2e	+51	3.8	1.16	+1.29	−0.60	−1.40	−2.14
192443.....	RS Cyg	C8, 2e	+ 3	0.6	0.21	+1.19	+0.12	−0.53	−0.67
206570.....	V460 Cyg	C6, 5	−13	0.5	0.14	+1.04	...	...	−0.25
223075.....	TX Psc	C6, 2	−56	0.4	0.13	−0.90	+0.09	−0.14	−0.36
			S Stars						
53791.....	R Gem	S3, 9e	+13	2.0	0.66	+1.74	−0.25	−0.98	−1.16
70276.....	V Cnc	S2, 9e	+28	0.3	0.18	−2.60	−0.12	−0.74	−1.03

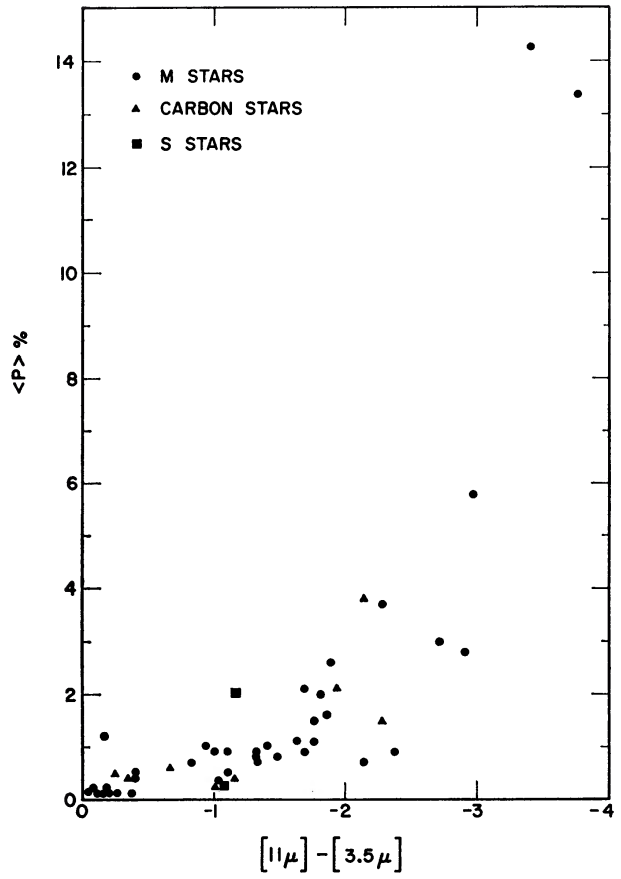

FIG. 1.—Average polarization as a function of the infrared color [11 μ] — [3.5 μ]. Not all of the data near the origin have been plotted.

Comparison of two stars—one unpolarized without significant infrared excess, and the other of the same temperature, polarized and with an infrared excess—seems to indicate that polarization is not a surface phenomenon. The correlation of polarization and surface temperature for an individual variable star is a natural feature of grain formation and does not affect this conclusion. Alternatively, a residual amount of gas may be present in the envelope regardless of whether the grains formed in the stellar atmosphere and were subsequently expelled by radiation pressure or formed, instead, in a preexisting circumstellar gaseous envelope. Kruszewski *et al.* (1968) have pointed out that the polarization in the envelope may be caused by Rayleigh scattering on atoms or molecules in the gas instead of by solid particles. The only requirement is that the gas be the main contributor to the opacity at visual wavelengths. However, under conditions in which an appreciable fraction of possible condensates exist as solids, scattering by the gas is small compared with scattering by the grains. Thus the observational evidence seems to indicate that solid particles are responsible for the measured intrinsic polarization in late-type stars.

It is remarkable that the correlation shown in Figure 1 is so good. Why are there not more stars with infrared excess that have only small amounts of intrinsic polarization? It might be expected that the varying geometrical aspect presented to the observer by a large number of stars would produce more scatter. This would be expected whether the polarization were caused by particles aligned in the envelope or by scattering from an asymmetric envelope of nonaligned particles. In contrast, most of the observed stars lie along a rather well-defined line in the ($\langle P \rangle$, [11.0 μ] — [3.5 μ])-diagram. Qualitatively,

this implies that, for most of the stars observed, the particles are concentrated in a strongly nonuniform shell around the star so that as the geometrical aspect to the observer changes from one star to another a rather asymmetric shell is still observed.

A comment about differences in chemical composition between observed stars should be made. Of the total number of stars that were observed in this work for polarization and infrared radiation, nine were classified normally as carbon stars. No significant difference in the correlation between intrinsic polarization and infrared excess was observed between M stars and carbon-rich stars. This implies that there is no significant characteristic of the polarization mechanism that is dependent on the chemical composition of the solid particles surrounding the star.

Finally, several other diagrams were plotted for the stars listed in Table 2. Only a weak correlation was found to exist between deviation of polarization from the average $\langle \Delta P \rangle$ as defined earlier and infrared excess [11 μ] − [3.5 μ]. Thus the degree of variability of the polarization has not yet been shown to have any relation to the measured intrinsic polarization or to the amount of infrared-emitting material surrounding the star. Further observations are needed to clarify this. A plot was also made of the measured intrinsic polarization versus the infrared excess, corrected for color attributable to the temperature differences between stars, $([11\ \mu] - [3.5\ \mu])_{\text{observed}} - ([11\ \mu] - [3.5\ \mu])_{\text{blackbody}}$. Almost no change at all was observed in the graph with this correction applied except for a minor shift of the infrared data to smaller excesses.

V. INTERPRETATION

As was discussed above, the observed relation between measured intrinsic polarization and infrared excess at $\lambda = 11\ \mu$ is surprisingly good. There is less scatter of the data below some upper boundary than one might expect when one considers that observations of many stars must include a great variety of geometrical aspects. In the Appendix a relation is derived which expresses the expected dependence of $\langle P \rangle$ on infrared excess of [11 μ] − [3.5 μ] under the now-proven hypothesis that solid particles surrounding late-type stars are responsible for both polarization and infrared excess. The relation arises because both polarization and amount of infrared emission are functions of optical depth: Intrinsic polarization is a function of the scattering optical depth of solid particles, and infrared excess is a function of the absorption optical depth of the grains. No assumption need be made about the exact mechanism that causes the polarization (i.e., aligned grains or asymmetric envelope) since an analysis based on absorption by aligned grains would be similar.

As is shown in the Appendix, the ratio of the observed flux at 11 μ to the flux at 3.5 μ can be expressed as

$$\frac{F_\lambda(11\ \mu)}{F_\lambda(3.5\ \mu)} = N + \frac{M(T)P}{[A/(1-A)]g + P},$$

where P = measured polarization; A = albedo = $Q_{\text{sca}}/Q_{\text{ext}} = \sigma_s/(\sigma_s + \sigma_a)$ where σ_s, σ_a are the particle scattering and absorption cross-sections; g = fraction of linear polarization of the total scattered light (the value lies between 0 and 1); N = constant; and $M = M(T)$ a slowly varying function of the effective temperature of the star.

In the case that the absorption optical depth of the envelope is very small, $\tau_a < 0.1$, which applied to most of the objects observed in this work since the amount of circumstellar infrared energy is small compared with the stellar energy, the ratio of 11-μ flux to 3.5-μ flux can be approximated by the linear relation

$$\frac{F_\lambda(11\ \mu)}{F_\lambda(3.5\ \mu)} = N + \frac{M(T)}{g}\left(\frac{1-A}{A}\right)P.$$

This linear relation should not apply to objects with optically thick circumstellar envelopes such as NML Cyg and VY CMa.

The numbers N and M in the above expression can be computed from available spectral data (Gillett, Low, and Stein 1968) as described in the Appendix. The constant g depends on the model taken for the scattering process leading to the observed polarization.

Figure 2 shows the measured average polarization plotted as a function of the ratio $F_\lambda(11\ \mu)/F_\lambda(3.5\ \mu)$ for comparison with the above derived linear relationship under the assumption that the number $M(T)$ is the same for all stars (same effective temperature for all stars). Except for a few exceptions such as χ Cyg and RW Cep, all of the stars with significant intrinsic polarization and significant infrared excess do not deviate far from the average effective temperature (if both spectral type and luminosity class are allowed for). Even those stars that are exceptions to this do not violate the approximate linear relationship greatly. This will for the present remain unexplained.

As a result of applying the theory developed in the Appendix to an asymmetric envelope model (Kruszewski *et al.* 1968), it has been deduced that the albedo of the scattering particles is rather high. The observed $\langle P \rangle$ versus infrared-excess data would be fitted by particles with albedo $A > 0.5$. No significantly different fit to the data was found for carbon stars than for M stars. Although the data at this time are rather crude, it is remarkable that as much information can be gained as has been shown here. Perhaps with more careful measurement techniques such as simultaneous polarization and

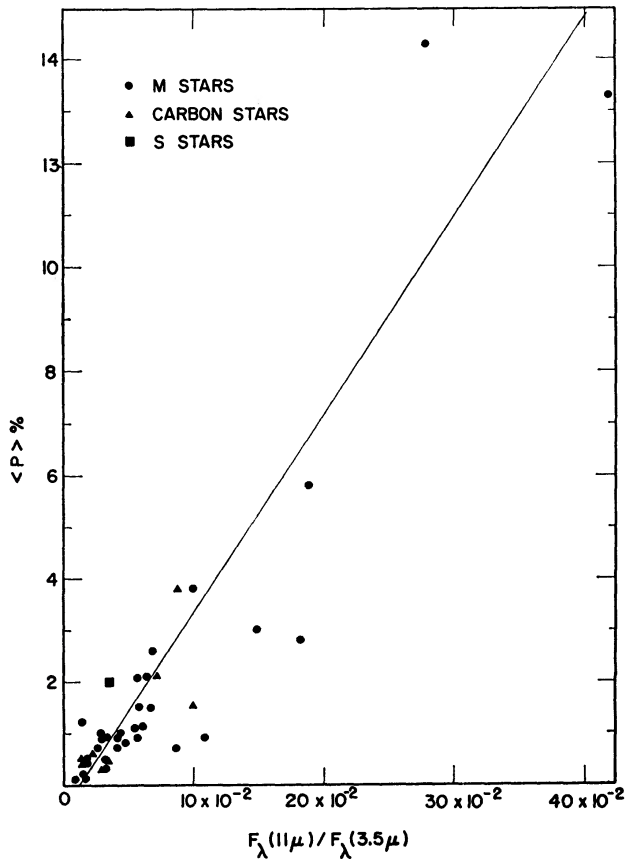

FIG. 2.—Average polarization as a function of $F_\lambda(11\ \mu)/F_\lambda(3.5\ \mu)$ for comparison with the approximate linear relationship derived in the Appendix. Note that the star RW Cep (K0 0b) lies to the right of the average line under the assumption that the value of $M(T)$ is the same for all stars. This is expected because RW Cep is considerably hotter than the other stars plotted. Not all of the data near the origin have been plotted.

infrared measurements, a more accurate determination of the properties of the individual particles and the geometrical properties of the circumstellar envelope may be found. It will be of particular interest to follow polarization and infrared excess simultaneously as a function of time for several of the subjects discussed here.

VI. CONCLUSIONS

A relation has been shown to exist between measured intrinsic polarization of late-type stars and infrared excess at $\lambda = 11\ \mu$. Except for a few objects, the observations cluster quite well along a rather well-defined line in the ($\langle P \rangle$, [11 μ] − [3.5 μ])-diagram. No difference was found in this relation between carbon stars and M stars. The expected dependence of $\langle P \rangle$ on infrared excess has been derived by relating intrinsic polarization to the scattering optical depth of a circumstellar envelope and the infrared excess to the absorption optical depth. As a result of this interpretation, it has been concluded that the albedo A of the particles as defined earlier in § IV is greater than 0.5. Further, more careful simultaneous observations of polarization and infrared excess will yield more specific information on the albedo of the particles and the physics of particles in the atmospheres of cool stars.

This work has been supported partially by the National Science Foundation and by NASA. Support was also contributed to N. J. W. and R. D. G. by the Graduate School of the University of Minnesota.

APPENDIX

In this Appendix we derive the dependence of the measured intrinsic polarization on the infrared excess of a circumstellar envelope of solid particles. The dependence is shown to occur through the scattering and absorption optical depths of the envelope.

Consider first the measured infrared flux at the two wavelengths of 11 and 3.5 μ. If the measured flux at 11 μ were due only to emission by solid particles with no contribution from the star, then the total flux of energy observed from the dust would be

$$F_T(\text{dust}) = F_0(T_*)(1 - e^{-\tau_a}) = [F_T(\text{dust}) + F(T_*)][(1 - e^{-\tau_a})] ,$$

where $F_0(T_*)$ = total flux from star if no dust present, $F(T_*)$ = total observed flux from star, and τ_a = absorption optical depth of the circumstellar envelope at optical wavelengths.

In photometric observations an approximate monochromatic flux is observed, and there are some spectral data (Gillett, Low, and Stein 1968) that allow a relation to be determined between the monochromatic measured flux and the total flux Thus the above equation yields the following type of expression for measured monochromatic flux:

$$\frac{F(3.5\ \mu)}{F(11\ \mu)} = \frac{1}{(e^{\tau_a} - 1)M(T)} ,$$

where $M(T)$ expresses the conversion factors between total flux observed from dust and measured monochromatic observed flux, as well as a similar conversion for measured 3.5-μ flux from the star and the total energy from the star. Now if the total optical depth of the envelope is very small at 11.0 μ, then a contribution of stellar energy will be observed at that wavelength. If this term is included, the observed ratio of flux at 3 5 μ to that at 11 μ is given by

$$\frac{F(3.5\ \mu)}{F(11\ \mu)} = \frac{1}{N + M(e^{\tau_a} - 1)} ;$$

and if $\tau_a \ll 1$, then

$$\frac{F(3.5\ \mu)}{F(11\ \mu)} = \frac{1}{N + M\tau_a} .$$

This analysis should not apply to objects with optically thick envelopes such as NML Cyg and VY CMa. However, it should apply to all other objects in this study.

Consider next the dependence of polarization on scattering optical depth. In general, the percent polarization P is of the form

$$P = \frac{I_{\max} - I_{\min}}{I_{\max} + I_{\min}},$$

where

$$I_{\min} = \tfrac{1}{2} I_* \exp(-\tau_T) + \tfrac{1}{2} I_u$$

and

$$I_{\max} = \tfrac{1}{2} I_* \exp(-\tau_T) + \tfrac{1}{2} I_u + I_p .$$

In these equations I_* = radiation emitted by star, I_u = unpolarized scattered light, I_p = polarized scattered light, and τ_T = total optical depth of envelope = $\tau_s + \tau_a$, where τ_s = scattering optical depth at optical wavelengths. Thus,

$$P = \frac{I_p}{I_* e^{-\tau_T} + I_s},$$

where I_s = total scattered light from envelope = $I_u + I_p$ The scattered-light contributions are given by expressions of the form $I_s = I_*(1 - e^{-\tau_s})$ and $I_p = g I_*(1 - e^{-\tau_s})$, where g is determined by the geometry of the scattering process. Consequently,

$$p = \frac{g}{1 + e^{-\tau_T}/(1 - e^{-\tau_s})} .$$

When the albedo $A = \tau_s/(\tau_s + \tau_a) = Q_{\rm sca}/Q_{\rm ext}$ is introduced, it can be shown that, under the conditions $\tau_T \ll 1$,

$$P = \frac{A(1 - A)^{-1} g \tau_a}{1 - \tau_a} .$$

Under most conditions considered here, τ_a is very small ($\tau_a < 0.1$); and unless $A \approx 1$, it can be shown that

$$\frac{F(11\ \mu)}{F(3.5\ \mu)} \approx N + \frac{M}{g}\left(\frac{1 - A}{A}\right) P .$$

The interpretation of the observed data in terms of the above derivation of the expected results is discussed in § V of the text.

REFERENCES

Coyne, G. V., and Kruszewski, A. 1968, *Ap. J.*, **73**, 20.
Donn, B., Stecher, T. P., Wickramasinghe, N. C., and Williams, D. A. 1966, *Ap. J.*, **145**, 949.
Dyck, H. M. 1968, *A.J.*, **73**, 688.
Dyck, H. M., and Jennings, M. C. 1971, to be published.
Dyck, H. M., and Sandford, M. T. 1971, to be published.
Gillett, F. C., Low, F. J., and Stein, W. A. 1968, *Ap. J.*, **154**, 677.
Gilman, R. C. 1969, *Ap. J.* (*Letters*), **155**, L185.
Harrington, J. P. 1969, *Ap. Letters*, **3**, 146.
Hoyle, F., and Wickramasinghe, N. C. 1962, *M.N.R.A.S.*, **124**, 417.
Kruszewski, A., Coyne, G. V., and Gehrels, T. 1969, in *Mass Loss from Stars*, ed. M. Hack (New York: Springer-Verlag).
Kruszewski, A., Gehrels, T., and Serkowski, K 1968, *A J*, **73**, 677.
Serkowski, K. 1966*a*, *Ap. J.*, **144**, 857.
——— 1966*b*, *I.A.U. Information Bull. Variable Stars*, p. 141.
———. 1969, *Ap. J.* (*Letters*), **156**, L139.
Shawl, S. J. 1969, *Ap. J.* (*Letters*), **157**, L57.
Woolf, N. J., and Ney, E. P. 1969, *Ap. J.* (*Letters*), **155**, L181.